Experimental study on perfobond strip connector in steel–concrete joints of hybrid bridges

Shaohua He [a], Zhi Fang [a,*], Yawei Fang [a], Ming Liu [a], Liyang Liu [b], Ayman S. Mosallam [c]

[a] College of Civil Engineering, Hunan University, Changha 410082, China
[b] Yunan Province Communications Planning and Design Institute, Kunming 650011, China
[c] Department of Civil and Environmental Engineering, University of California, Irvine, CA 92697-2175, USA

ABSTRACT

Perfobond strip (PBL) connectors, consisting of a perforated steel plate with steel rebar passing through the holes and embedded in concrete to transfer the shear action between the concrete and steel components, are increasingly used in composite and hybrid girders and columns. Though many studies on the behavior of PBL connectors can be found in the literature, the load transferring mechanism of PBL still needs further clarification because noticeable discrepancies can be found among the existing equations for predicting the shear capacity of the connectors. This paper presents an experimental study of the structural response of PBL connectors under push-out loading. Twelve push-out specimens fabricated according to the design used for the connectors in the steel–concrete joints in a hybrid cable-stayed bridge have been investigated. The behavior of the connectors, including the failure modes, ductility, and the components of the ultimate shear-resistant capacity, is discussed in depth. The results indicate that the mechanical properties of the PBL specimens are improved due to the bond at the interface between the perforated plate and the concrete. The transverse rebar located in the center of the steel plate hole is important for ensuring the connector's ductility. Furthermore, an analytical model and corresponding equation for predicting the ultimate resistance of PBL connectors with shear failure of the dowel are proposed, and the feasibility of the developed equation has been verified by the experimental results from related references.

© 2015 Elsevier Ltd. All rights reserved.

1. Introduction

Steel–concrete composite and hybrid structures have been widely used in civil engineering, and shear connectors are the most important element for the transmission of force between steel and concrete. The headed stud is the most commonly used shear connector in structures because it can be automatically welded and produced on a large scale. However, with their wide use in bridges, the fatigue problem of the studs becomes serious [1]. An alternative new connector, called the perfobond strip (PBL), consisting of a perforated steel plate with steel rebar passing through the holes and embedded in concrete to transfer the shear action between the concrete and steel components, was introduced in 1987 [2]. The shear resistance of PBL is comprised of the bonding effects at the interface between the perforated steel plate and concrete, the resistance of the concrete dowel, the resistance of the transverse rebar passing through the holes in the steel plate and the local bearing effects between the end of the steel plate and the concrete. PBL connectors have been widely used in composite structures, particularly in the composite beams and steel–concrete joints of hybrid girder bridges.

The performance of PBL connectors in composite beams has been extensively studied through push-out tests with the standard separated type of specimen recommended in EC. 4 [3] and as shown in Fig. 1(a). Because the effort of separation between the steel girder and the concrete slab caused by the bending moment in composite beams cannot be ignored, lubricating oil is required on the steel flange to eliminate the bonding effect and possible friction in the standard push-out test procedure. The failure mode of PBL by standard push-out tests in previous studies was commonly controlled by the cracking of a concrete slab [4–17].

By comparison, the PBL in a steel–concrete joint of a hybrid bridge is embedded in a thick concrete block, and its failure generally results from the fracture of the dowel of concrete and the transverse rebar caused by the holes on the steel plate. No uplift force is found between the perforated plate and the concrete, and the bonding effects at the interface between the steel plate and the concrete could make a contribution to the shear strength of the connectors. Meanwhile, because a sufficient quantity of PBL is usually adopted to transfer the enormous shear force between the steel components and the concrete in hybrid joints, the effects of the local concrete at the end of the perforated plate are negligible [18]. As a result, the differences between the load transferring mechanism of PBL in steel–concrete joints and composite beams are significant.
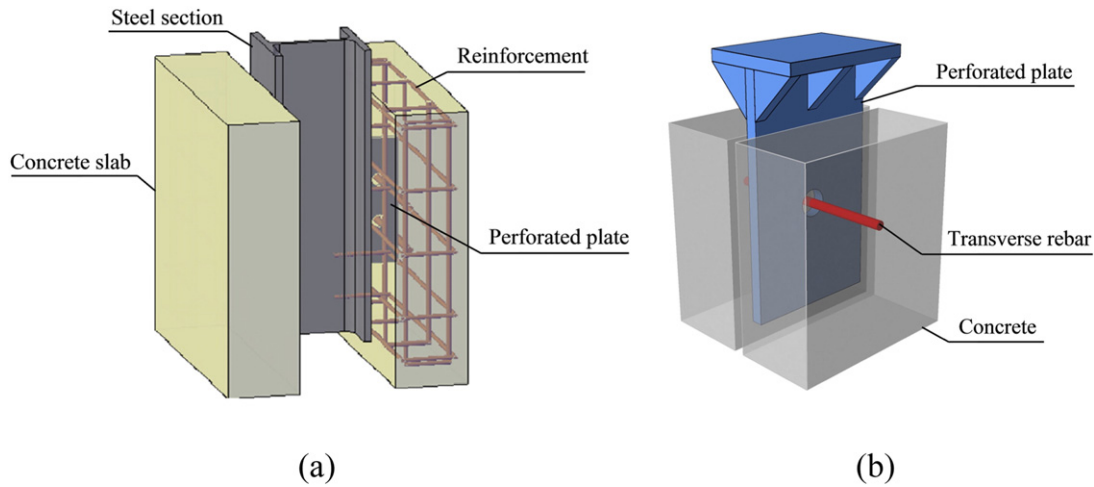
Fig. 1. The push-out test model: (a) The separated type of push-out specimen; (b) The plug-in type of push-out specimen.

As the failure of PBL in steel–concrete joints differs from the connectors in composite beams, the push-out test with the separated type of specimen is not appropriate for simulating the failure mode of PBL connectors in hybrid joints. Su et al. [19] suggested a push-out test procedure, using the plug-in type of specimen composed of a concrete block and a single perforated steel plate with transverse rebar passing through the hole, as shown in Fig. 1(b), to simulate the performance of the PBL in the steel–concrete joints of hybrid girder bridges. On the bottom of the specimen there is no support at the end of the steel plate to eliminate the local bearing for the steel plate. This plug-in type of push-out specimen was used by Q.H. Zhang et al. [20], L. Xiao et al. [21] and W.M. Wu [22] to study the behavior of PBL with the shear failure modes of the concrete and/or transverse rebar dowels crossing the holes in the steel plate.

The recently completed Nujiang bridge, as shown in Fig. 2(a), located in Yunan, China, with a single pylon and a single cable plane as well as a span arrangement of 81 m + 175 m, is a cable-stayed bridge with a hybrid girder consisting of three parts: the Prestressed Concrete (PC) girder, the steel girder and a 2 m long steel–concrete composite joint. The joint is composed of a steel back bearing plate and several steel cells filled with concrete, and PBL connectors are installed in the steel cells to transfer the shear force between the concrete and the steel plates, as shown in Fig. 2(b) to (d). Based on the geometric configuration of the connectors in this bridge, a test was conducted to simulate the mechanical properties of PBL connectors in steel–concrete joints.

Though there have been studies of PBL in steel–concrete joints, few were focused on the bonding effects at the interface between the perforated plate and the concrete or on its load transferring mechanism in hybrid joints. In this paper, the push-out test using the plug-in type specimen is introduced, and based on the experimental results, the effects of the interface bond, the dowels of concrete and the transverse rebar in the hole on the properties of PBL, as well as the suitability of the existing equations for predicting the resisting capacity of PBL are
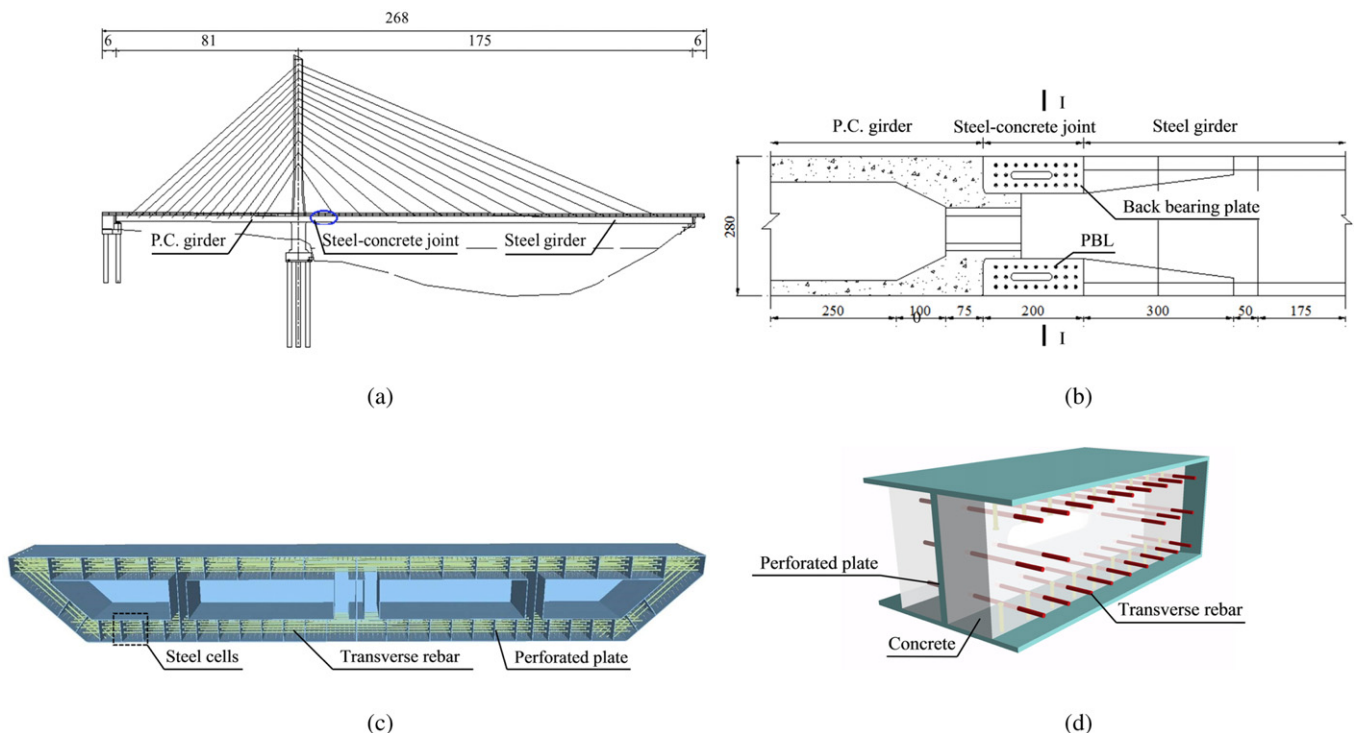

Fig. 2. Nujiang bridge: (a) Elevation view (unit: m); (b) Steel–concrete joint part (unit: cm); (c) Section of I–I; (d) PBL connectors in the steel cells.

discussed; and finally, an analytical equation for the capacity prediction of PBL regarding the shear failure modes of the concrete and/or transverse rebar dowels through the holes is developed and verified by experimental results.

2. Experimental details

2.1. Specimen design

The test parameters in this work include the bond state of the steel plate surfaces, the type of dowel passing through the hole and the interaction of the bond and dowels. The 12 tested plug-in type push-out specimens, as shown in Fig. 1(b) and in Table 1, were divided into 6 groups with 2 identical samples of each group. The 6 groups of specimens were: the pure bond specimen, unbonded concrete dowel specimen, bonded concrete dowel specimen, bonded rebar specimen, unbonded PBL specimen and standard PBL specimen. The pure bond specimens were utilized to investigate the bonding effect at the interface between the steel plate and the concrete; the unbonded concrete dowel specimens were used to study the shear capacity of concrete dowel by the hole; the bonded concrete dowel specimens were used to explore the combined action of the bond and concrete dowel; the bonded rebar specimens were used to study the combination of the bond and transverse rebar in shear; the unbonded PBL specimens were used to investigate the interaction of the concrete dowel and the transverse rebar near the hole and the standard PBL specimens were used to explore the compound action of the interface bond, concrete dowel and transverse rebar near the hole.

In the specimen codes shown in Table 1, C represents C50 normal concrete; b, r, and d represent the interface bond, the transverse rebar and the concrete dowel near the hole, respectively, and the number 1 or 0 after the b, r, or d indicates whether the corresponding part exists, with 1 for Yes and 0 for No. For example, "C-b1r0d1" indicates a specimen fabricated using C50 normal concrete with the interface bond and the concrete dowel near the hole but without the transverse rebar passing through the hole.

Fig. 3 shows the detailed dimensions of the specimens, in each of which a steel plate, with a nominal yield stress of 345 MPa, width × height × thickness of 300 mm × 555 mm × 25 mm, a circular hole with diameter of 21 mm for C-b1r1d0 and 60 mm for the others (except for specimen C-b1r0d0 without any holes on its steel plate), is plugged into the concrete block, and a 20 mm-diameter transverse rebar with a nominal yield stress of 335 MPa was placed through the hole for those specimens with the transverse rebar.

2.2. Material properties

Tables 2 and 3 show the properties of the concrete and reinforcement for the specimens, respectively. The cubic compressive strength of the concrete was measured on 150 mm × 150 mm × 150 mm cubes, and the prismatic strength and elastic modulus of the concrete were measured on 150 mm × 150 mm × 300 mm prisms; HPB235 rebar with a diameter of 10 mm and nominal yield strength of 235 MPa was used as the primary reinforcement for the concrete

block, and HRB335 rebar with a diameter of 20 mm and nominal yield strength of 335 MPa was used as the transverse rebar in the hole.

2.3. Test layout and instrumentation

All the tests were performed in a universal testing machine with a capacity of 2000 kN, as shown in Fig. 4(a). The relative slip between the steel plate and the concrete block was measured by the 2 linear variable differential transformers (LVDTs) installed on the 2 opposite sides of the concrete block, as shown in Fig. 4(b). The loading process complied with the procedure recommended in EC. 4. First, a cyclic load ranging from 5% to 40% of the expected failure load was applied at the rate of 5 kN/s for 25 cycles, then a monotonic load controlled by the relative slip between the steel and concrete was applied until failure of the specimens in not less than 15 min.

3. Test results and discussion

3.1. General results

Table 4 shows the ultimate load V_u and the relative ultimate slip S_u. Here we defined the maximum load experienced V_u and the slip S_u at V_u as the ultimate load and ultimate slip, respectively. The ultimate loads and slips, especially the ultimate loads, of the 2 different specimens in each group are relatively close. As such, the subsequent description of the behavior of the specimens in each group will be based on the average values of the 2 specimens in the group.

For those specimens with a hole in the steel plate, the dowel near the hole was finally shorn off at the ultimate load, as indicted in other similar studies [18–22]. For the specimens without the transverse rebar through the hole, such as the pure bond specimens in group C-b1r0d0 and the bonded and unbonded concrete dowel specimens in groups C-b1r0d1 and C-b0r0d1, few cracks were found on the surfaces of the concrete block, as shown in Fig. 5(a) due to the smaller slip at the ultimate load; however, for the specimens with the transverse rebar in the hole, such as the bonded rebar specimens in group C-b1r1d0, the unbonded PBL specimens in group C-b0r1d1 and the standard PBL specimens in group C-b1r1d1, more and wider cracks could be seen on the concrete block, as shown in Fig. 5(b), resulting from the larger steel plate slip at the ultimate load.

All concrete blocks were cut off after testing to observe the state of the dowels in the hole. For group C-b1r1d0, with a rebar of 20 mm diameter in a hole in the plate of 21 mm diameter and with almost no concrete dowel surrounding the rebar, the transverse rebar was shorn off directly at the interface between the steel plate and the concrete, as shown in Fig. 5(c). In comparison, for groups C-b0r1d1 and C-b1r1d1, with a rebar of 20 mm diameter in a much larger hole of 60 mm diameter in the plate and thus with a concrete dowel surrounding the rebar, the failure mode of the transverse rebar within the concrete dowel could be attributed to fracture under the bend–shear interaction, and thus a much larger plastic deformation before failure was found in these specimens, as shown in Fig. 5(d).

Table 1
Specimen characteristics.

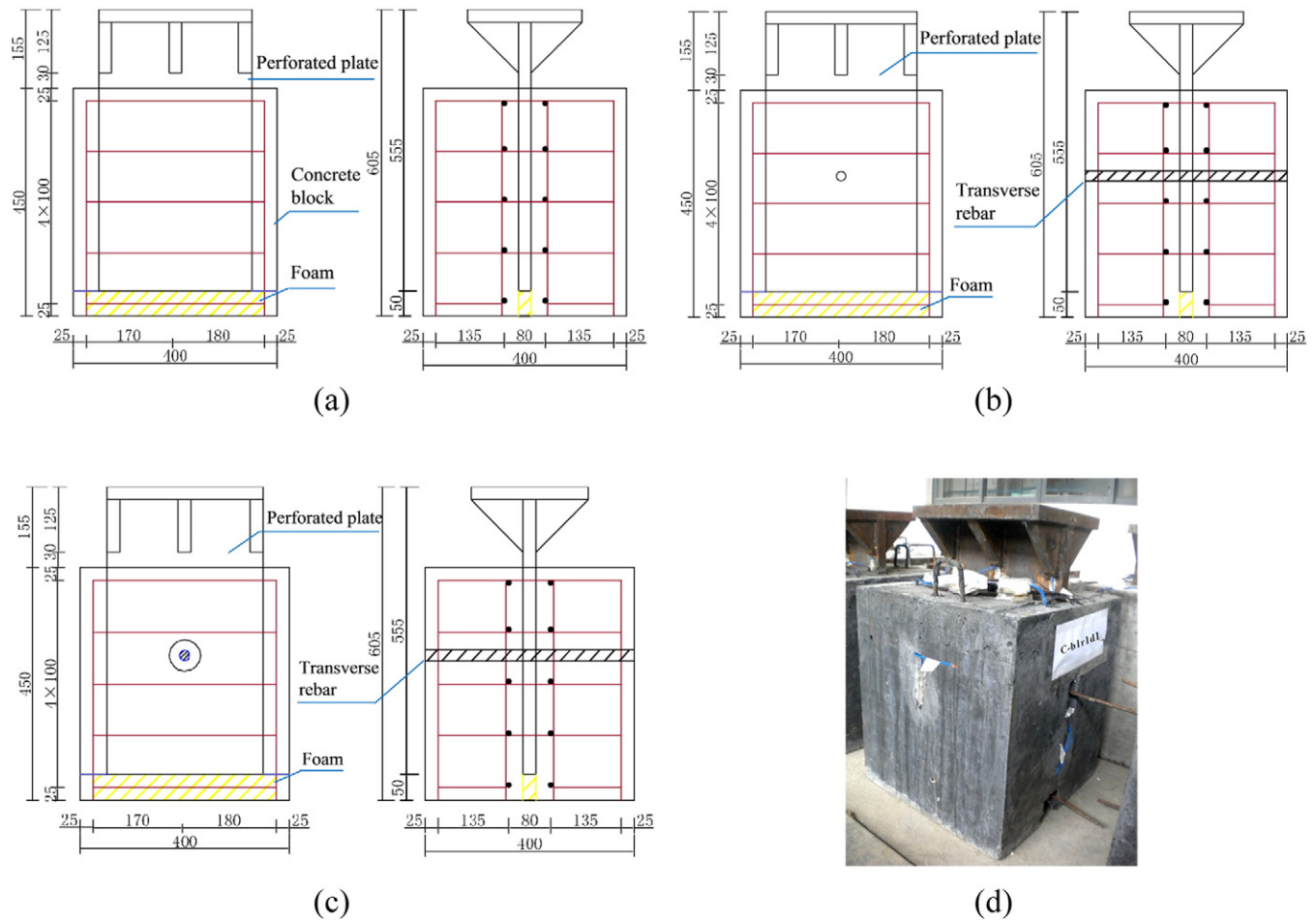| Group No.	Specimen code	State	Components of resistance			Diameter of the hole (mm)	Diameter of transverse rebar (mm)
			Bond	Concrete dowel	Transverse rebar		
1	C-b1r0d0	Pure bond	√			–	–
2	C-b0r0d1	Unbounded concrete dowel		√		60	–
3	C-b1r0d1	Bonded concrete dowel	√	√		60	–
4	C-b1r1d0	Bonded rebar	√		√	21	20
5	C-b0r1d1	Unbonded PBL		√	√	60	20
6	C-b1r1d1	Standard PBL	√	√	√	60	20

Fig. 3. Structural layout of the specimens: (a) C-b1r0d0; (b) C-b1r1d0; (c) C-b1r0d1 and C-b1r1d1; (d) Specimen for testing.

3.2. Load–slip curves

Fig. 6 shows the load–slip curves for all the specimens in this study. As plotted in the figures, those specimens without transverse rebar experienced a maximum slip of 1.91 mm at the ultimate load, which is much smaller than the required slip capacity of 6 mm for a ductile connector in EC. 4 [3]. In comparison, all specimens with transverse rebar in the hole demonstrated a ductile behavior because all had slip at the ultimate load greater than 6 mm.

Fig. 6(a) shows the load–slip curves for the 2 pure bond specimens in group C-b1r0d0. The average ultimate load and slip in the group were 302 kN and 0.61 mm, respectively; and the residual load capacity of the interface friction was approximately 141 kN and remained nearly constant. The bond stresses on the interface between the steel plate and concrete at the ultimate and residual loads were 1.06 MPa and 0.51 MPa, respectively.

Fig. 6(b) and (c) presents the load–slip curves for the unbonded and bonded concrete dowel specimens in groups C-b0r0d1 and C-b1r0d1, respectively. For the specimens with only the concrete dowel, group C-b0r0d1, the average ultimate load and slip at the concrete dowel fracture were 247 kN and 0.82 mm, respectively, and the residual load

capacity of the friction on the fractured dowel interface was approximately 173 kN. In comparison, for the specimens with both the interface bond and concrete dowel, group C-b1r0d1, the average ultimate load and slip at dowel fracture were 370 kN and 1.91 mm, respectively, and the residual load capacity of the friction on the interface was approximately 291 kN. It is seen that the residual load difference between groups C-b0r0d1 and C-b1r0d1, which is caused by the friction at the plate surface, is 118 kN. Due to the effect of the interface bond, the ultimate load and slip of group C-b1r0d1 increased by 50% and 133%, respectively, compared to group C-b0r0d1.

Fig. 6(d) is the load–slip curves for the specimens in group C-b1r1d0 with both the interface bond and rebar dowel but without the concrete dowel, in which a 20-mm-diameter rebar was set in a 21-mm-diameter hole in the plate and with almost no concrete dowel surrounding the rebar. The average ultimate load and slip at the rebar dowel fracture were 326 kN and 6.81 mm, respectively. According to the compatibility of the slip deformation between the specimens in groups C-b1r1d0 and C-b1r0d0, at the ultimate slip of 6.81 mm in C-b1r1d0, the shear-resistant capacity of the friction on the steel plate interface should be approximately equal to 141 kN, which was the residual load capacity of the pure bond specimens in group C-b1r0d0. As such, the shear-resistant capacity supplied by the rebar dowel was approximately 185 kN. Comparing the results of group C-b1r1d0 with those of group C-b1r0d0, although the ultimate load only increased slightly by 8% because the maximum shear-resistant capacity separately provided by the interface bond and rebar dowel could not occur simultaneously, the slip at the ultimate load increased by 11 times. It was obvious that the deformability of the connectors resulted from the transverse rebar near the hole. Additionally, according to the tensile strength of

Table 2
Properties of the concrete.

Type	Nominal strength (MPa)	Cubic compressive strength (MPa)	Prismatic strength (MPa)	Elastic modulus (GPa)
C50	50	58.1	46.1	37.2

Table 3
Properties of the reinforcements.

Diameter (mm)	Grade	Yield strength f_y (MPa)	Tensile strength f_u (MPa)	Elastic modulus E (GPa)	Elongation rate δ (%)
10	HPB235	286	446	201	25
20	HRB335	388	549	207	26

549 MPa for 20-mm-diameter rebar, the theoretical ultimate capacity under pure or direct shear with two symmetric shear failure faces for the rebar is 199 kN. Although it is slightly larger than the value of 185 kN deduced above, the two could be viewed as close considering that only a single shear face occurred in the latter, resulting from the fact that an ideal symmetric shear failure was actually impossible. As such, it is appropriate to conclude that the failure at ultimate load of the rebar with almost no concrete dowel surrounding it in the specimens of group C-b1r1d0, as shown in Fig. 5(c), was due to direct shear.

Fig. 6(e) and (f) shows the load–slip curves for the unbonded and standard bonded PBL specimens in groups C-b0r1d1 and C-b1r1d1, respectively. For the unbonded PBL specimens in group C-b0r1d1 with the reinforced concrete dowel but without the interface bond and a 20-mm-diameter rebar with a surrounding concrete dowel in a 60-mm-diameter hole in the plate, the average ultimate load and slip at the dowel fracture were 449 kN and 14.16 mm, respectively. In comparison, for the standard PBL specimens in group C-b1r1d1 with the interface bond and the same reinforced concrete dowel, the average ultimate load and the corresponding slip were 547 kN and 17.65 mm, respectively. Obviously, with the interface bond, the ultimate load and slip of group C-b1r1d1 are 22% and 25% higher, respectively, than those of group C-b0r1d1.

Moreover, comparing the results of the unbonded PBL specimens in group C-b0r1d1 with those of the unbonded concrete dowel specimens in group C-b0r0d1, it can be found that a 20-mm-diameter rebar inside the concrete dowel would result in the ultimate load and slip increasing by 82% and 17 times, respectively. Similarly, a comparison of the results between the standard PBL specimens in group C-b1r1d1 and the bonded concrete dowel specimens in group C-b1r0d1 indicates that providing a rebar inside the concrete dowel can increase the ultimate load and slip by 48% and 10 times, respectively. It is apparent that for both the bonded and unbonded PBL specimens, the bulk of the ultimate deformability was contributed by the action of the transverse rebar inside the concrete dowel.

Additionally, compared to the bonded rebar specimens in group C-b1r1d0 with a 20-mm-diameter rebar in a 21-mm-diameter hole in the plate and with almost no concrete dowel surrounding the rebar, the ultimate load and slip at the dowel fracture of the standard PBL specimens in group C-b1r1d1, with a rebar of 20 mm diameter in a much larger hole of 60 mm diameter in the plate and thus with a concrete dowel surrounding the rebar, increase by 68% and 2.6 times, respectively. As such, although the failure modes of the specimens in the two groups C-b1r1d0 and C-b1r1d1 all resulted from fracture of the transverse rebar, the ultimate load and slip in the latter were improved largely because the transverse rebar in the latter was fractured under the bend–shear interaction rather than direct shear due to the support and confinement effect of the concrete dowel outside its transverse rebar. Similarly, according to the compatibility of the slip deformation of the specimens in groups C-b0r1d1 and C-b0r0d1, at the ultimate slip of 14.16 mm of C-b0r1d1, the shear-resistant capacity by the concrete dowel action in C-b0r1d1 should be approximately 175 kN, which was the residual load capacity of the pure concrete dowel specimens in group C-b0r0d1 at the ultimate slip of 14.16 mm; further, the corresponding shear-resistant capacity supplied by the rebar dowel in the C-b0r1d1 specimens was approximately 274 kN (calculated as the ultimate load of 449 kN of the C-b0r1d1 specimens minus 175 kN), which is much larger than the value of 185 kN of the rebar dowel contribution in the C-b1r1d0 specimens without any concrete dowel surrounding the rebar due to the bending-shear failure rather than the direct shear failure in the rebar dowel in C-b0r1d1.

3.3. Constitutive analysis of the shear-resistant capacity in PBL connectors

Fig. 7 shows the load–slip curves of the different specimens from groups C-b1r1d1, C-b1r0d1, C-b0r0d1 and C-b1r0d0 simultaneously so that the shear-resistant capacity constitution of a PBL connector can be explained explicitly.

Regarding the standard PBL specimen in group C-b1r1d1, its shear-resistant capacity is a combination of the interface bond and the shear resistance of the concrete and transverse rebar dowels through the hole in the steel plate. The contribution of each part can be found from the load–slip curves of the relative specimens shown in Fig. 7.

The average ultimate load and slip of the specimens in group C-b1r1d1 were 547 kN and 17.65 mm, respectively. According to the
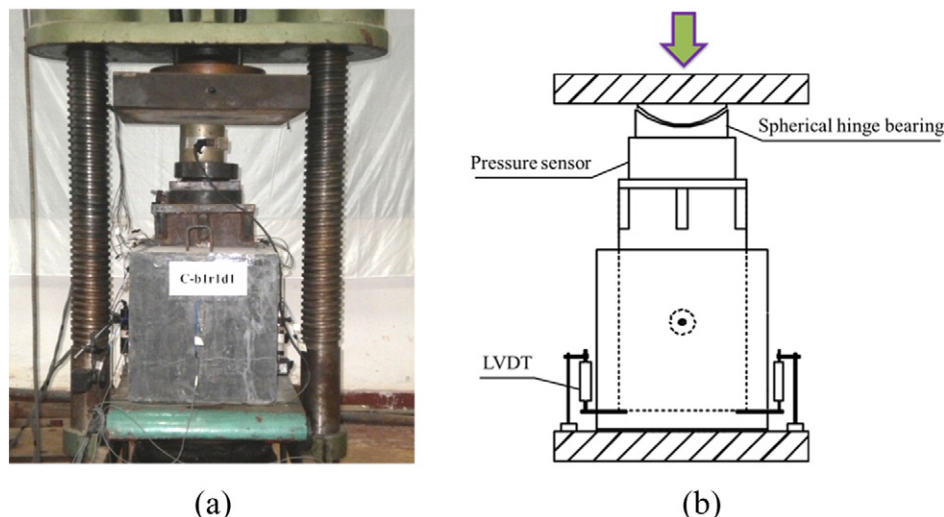

Fig. 4. Push-out test setup: (a) General layout and equipment; (b) Layout of LVDTs.

Table 4
Static experimental results.

| No.	Specimen Code	Ultimate load V_u (kN)			Slip at ultimate load S_u (mm)			Failure modes
		Spe.-1	Spe.-2	Ave.	Spe.-1	Spe.-2	Ave.	
1	C-b1r0d0	309	294	302	0.56	0.66	0.61	Shear failure at the interface
2	C-b0r0d1	232	261	247	0.71	0.93	0.82	Shear failure of concrete dowel in the hole
3	C-b1r0d1	359	381	370	2.18	1.63	1.91	Shear failure of concrete dowel in the hole
4	C-b1r1d0	324	327	326	7.24	6.38	6.81	Shear failure of transverse rebar in the hole
5	C-b0r1d1	446	452	449	14.70	13.61	14.16	Shear failure of the dowels in the hole
6	C-b1r1d1	543	551	547	17.10	18.20	17.65	Shear failure of the dowels in the hole

compatibility of the slip deformation among the specimens in groups C-b1r0d0, C-b0r0d1 and C-b1r0d1, at the ultimate slip of 17.65 mm of C-b1r1d1, the shear-resistant capacity of the friction on the steel plate interface should be approximately equal to 141 kN, which is the residual load capacity of the pure bond specimens in group C-b1r0d0 at the slip of 17.65 mm; the capacity of the concrete dowel should be approximately 154 kN, which is obtained on the basis of the residual load capacity of 173 kN of the unbonded concrete dowel specimens in group C-b0r0d1 but considering the reduction in area occupied by the rebar in the concrete dowel in the standard PBL specimens in group C-b1r1d1; further, the capacity of the transverse rebar inside the concrete dowel could be approximately determined as 256 kN, which is the load difference between groups C-b1r1d1 and C-b1r0d1 at the slip of 17.65 mm. As such, the sum of the three separate components — the interface friction, concrete dowel and rebar — was 551 kN, which is almost equal to the measured ultimate load of 547 kN for C-b1r1d1.

Using the same method, each component of the shear-resistant capacity of the bonded concrete dowel specimen in group C-b1r0d1 could also be obtained, as summarized in Table 5. A good agreement between the measured and the estimated shear resistance was found, which indicates that the shear resistance of a PBL connector could be obtained by adding the contributions of the interface bond, the concrete and the transverse rebar dowels on the basis of the compatibility of the slip deformation at the ultimate load. It also can be observed that the shear resistance provided separately by the interface bond, the concrete dowel and the transverse rebar accounted for 26%, 28% and 46%, respectively, of the overall capacity in the present standard PBL connector.
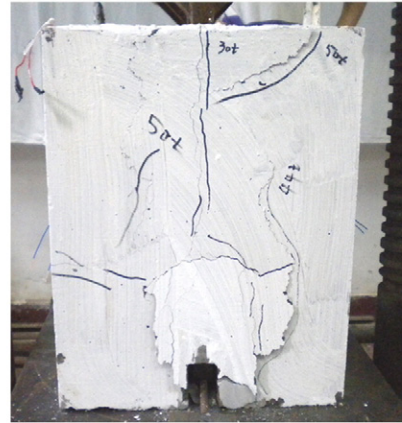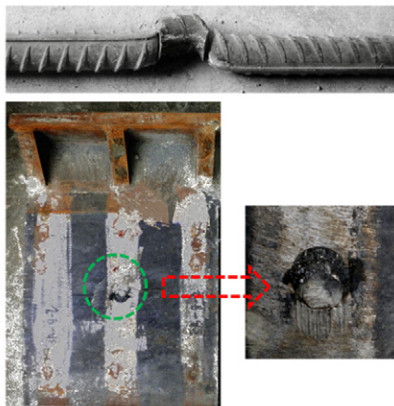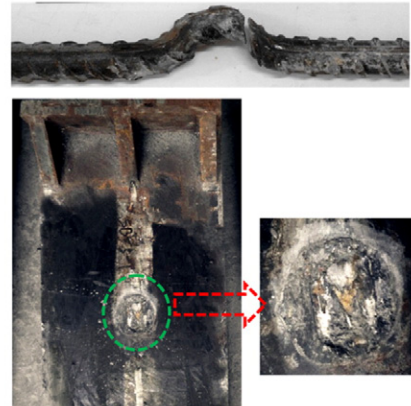

Fig. 5. Failure of the push-out specimens: (a) Crack distribution in specimens without transverse rebar; (b) Crack distribution in specimens with transverse rebar; (c) Failure of transverse rebar in group C-b1r1d0; (d) Failure of transverse rebar in groups C-b0r1d1 and C-b1r1d1.
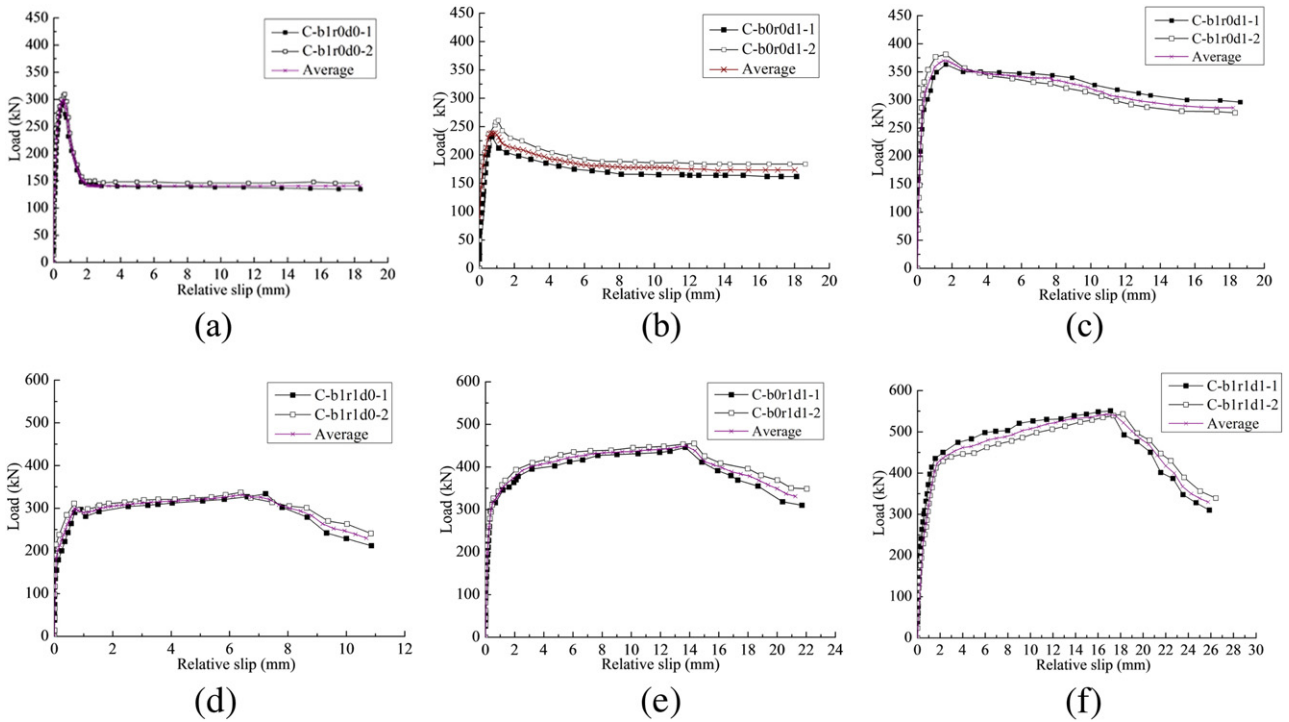
Fig. 6. Load–slip curves for different connector types: (a) Pure bond specimen; (b) Unbonded concrete dowel specimen; (c) Bonded concrete dowel specimen; (d) Bonded rebar specimen; (e) Unbonded PBL specimen; (f) Standard PBL specimen.

4. The equations for the shear-resistant capacity of the PBL

4.1. The existing equations

A number of equations for predicting the shear-resistant capacity of PBL have been developed by different researchers [2,4,6,7,9,11,12], and some typical ones are listed in Table 6.

Table 7 presents a comparison of the test results from the present work and the calculated results from the equations in Table 6. In Table 7, the numerator indicates the test or the calculated shear resistance, and the denominator is the relevant predictive error between the calculated and the experimental results.

It can be seen from the results of the comparison shown in Table 7 that the shear-resistant capacity of the PBL connectors from the present test can only rarely be predicted well by the existing equations listed in Table 6. In the case of the standard PBL specimens in group C-b1r1d1, the relevant predictive errors by those equations ranged from 19%–51%, and those for the unbonded PBL specimens in group

Fig. 7. Analytical diagrams of the standard PBL.

C-b0r1d1 ranged from 1%–40%. As such, it is imperative to develop a more applicable model to provide better capacity estimation for the PBL connectors in the steel–concrete joints of hybrid bridges.

The perfobond connector was first developed by Leonhardt et al. [2] and Hans-Peter [4], and in the original design of the connector, the transverse rebar through the hole was not a necessary component; thus, the equations proposed by Leonhardt et al. [2] and Hans-Peter [4] did not include the effect of the transverse rebar. The failure of the specimens in their experimental research was due to the yield of the steel component between the two adjacent holes. As such, the equations proposed cannot predict the capacity well for the present specimens.

In the expressions proposed by Oguejiofor and Hosain [6], Ahn et al. [7], Al-Darzi et al. [9], and Vianna et al. [11], the contribution of the local bearing of the concrete at the end of the steel plate was considered. However, for those multiple PBL in a series layout in the steel–concrete joints of hybrid girder bridges, the influence of the local bearing due to the concrete at the end of the steel plate on the capacity is negligible [18], and as such, the local bearing effect is eliminated in the present test. As shown in Table 7, the capacity calculated by these equations [6,7,9,11] but without considering the effect of the local bearing is far lower than the actual values obtained for the connectors in the test. Additionally, the failure of push-out specimens tested by these researchers [6,7,9,11] also occurred in the concrete slabs.

The equation suggested by Hosaka et al. [12] was based on the test results from standard push-out specimens as shown in Fig. 1(a) that generally experienced a failure of the concrete slabs next to the steel component, whereas the failure mode of the plug-in type push-out specimen shown in Fig. 1(b) in the present work mainly resulted from dowel fracture. Therefore, the capacity of the present specimens cannot be estimated well by the equations developed by Hosaka et al. [12].
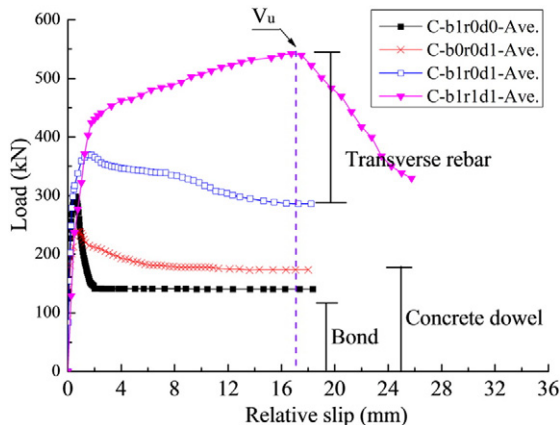
4.2. The proposed equation

Because the shear capacity of the PBL connectors in the steel–concrete joints of hybrid bridges cannot be evaluated well by the

Table 5
Components of connector shear resistance.

Specimen code	Measured shear resistance (kN)	Contribution of each part (kN)			Estimated shear resistance (kN)	Measurement/Estimation
		Interface bond	Concrete dowel	Transverse rebar		
C-b1r1d1	547	141	154	256	551	0.99
C-b1r0d1	370	161	221	0	382	0.97

existing equations mainly for the PBL connectors in composite beams, a more applicable model is necessary for predicting the shear capacity of PBL connectors in the case of dowel fracture as the failure mode.

Considering that the shear capacity of a PBL connector could be achieved by adding the contributions of the interface bond, the concrete and the transverse rebar dowels on the basis of the compatibility of the slip deformation at the ultimate load, as mentioned above, the ultimate shear capacity of a standard PBL connector is assumed to be as in Eq. (1).

$$V_u = V_{bv} + V_{cv} + V_{sv} \tag{1}$$

where:

V_u The ultimate resistance of a PBL connector;
V_{bv}, V_{cv} and V_{sv} The resistance of the interface bond on the steel plate surface, concrete and transverse rebar dowels in the hole, respectively and were determined as follows.

I) The resistance of the interface bond

The resistance of the interface bond between steel plate and the concrete can be defined as

$$V_{bv} = \tau_b A_b \tag{2}$$

where:

τ_b The bonding strength between the steel plate and the concrete (MPa);
A_b The area of the contact surface between the steel plate and the concrete (mm^2).

The expression for the bonding strength between the flat steel plate and the concrete can be obtained as [23]:

$$\tau_u = -0.054 f_{cu} + 0.7\sqrt{f_c'} - 1.193 \tag{3}$$

where:

τ_u The ultimate bonding strength between the steel plate and the concrete (MPa);
f_c' The cylindrical concrete compressive strength (MPa).

Considering the relation between the cubic and the cylindrical compressive strength, with $f_c' = 0.83 f_{cu}$ as in reference [24], Eq. (3) can be expressed as

$$\tau_u = -0.045 f_{cu} + 0.638\sqrt{f_{cu}} - 1.193 \tag{4}$$

where:

f_{cu} The cubic compressive strength of the concrete (MPa).

With the help of the model CEB-FIP MC90 [25] for the bond–slip relation between the rebar and the surrounding concrete, as shown in Fig. 8(a), and the test results from the pure bond specimens in group C-b1r0d0 in present study, the bond–slip curve between the flat steel plate and the concrete is developed as Eq. (5) and shown in Fig. 8(b).

$$\tau_b = \begin{cases} \tau_u \left(\dfrac{s}{0.61}\right)^{0.29} & 0 \le s \le 0.61 \\ \tau_u (1.24 - 0.47s) & 0.61 < s \le 1.65 \\ 0.48\tau_u & 1.65 < s \end{cases} \tag{5}$$

where s is the slip between the steel plate and the concrete (mm).

As indicted above, the ultimate slip of the standard PBL is much larger than 1.65 mm, and as such, the bonding strength of the steel plate/concrete interface at the ultimate load of a standard PBL can be obtained from Eq. (5) as follows:

$$\tau_b = -0.022 f_{cu} + 0.306\sqrt{f_{cu}} - 0.573. \tag{6}$$

II) The resistance of the concrete dowel in the hole

The load state of the concrete dowel is illustrated in Fig. 9, where σ_A is the compressive stress from the steel plate, σ_B is the supporting stress of section B, σ_c is the lateral compressive stress from the concrete blocks alongside, and I–I is the fracture section of the concrete dowel.

The contribution of the concrete dowel resistance shown in Fig. 9(c) can be calculated by

$$V_{cv} = 2\tau_{cv} A_c \tag{7}$$

Table 6
Some typical models for the shear resistance of PBL.

Authors	Predicting models		Notation
Leonhardt et al. [2]	$V_u = 2.553 D^2 f_c'$		V_u: Shear capacity of connector
Hans-Peter [4]	$V_u = 2.257 D^2 f_c'$		D: Diameter of the hole
Oguejiofor and Hosain [6]	$V_u = 4.5 h_{sc} t_{sc} f_c' + 0.91 A_{tr} f_y + 3.31 n D^2 \sqrt{f_c'}$		f_c': Cylindrical concrete strength
Ahn J.H. et al. [7]	$V_u = 3.14 h_{sc} t_{sc} f_c' + 1.21 A_{tr} f_y + 1.895 n\pi D^2 \sqrt{f_c'}$		h_{sc}: Height of connector
			t_{sc}: Thickness of connector
Al-Darzi et al. [9]	$V_u = 255.31 + 7.62 \times 10^{-4} h_{sc} t_{sc} f_c' - 7.59 \times 10^{-7} A_{tr} f_y + 2.53 \times 10^{-3} A_{sc} \sqrt{f_c'}$		A_{tr}: Area of transverse rebars
Vianna J.C. et al. [11]	$V_u = 31.8 + 1.9 \times 10^{-3} h_{sc} t_{sc} f_c' + 0.53 \times 10^{-3} A_{tr} f_y - 0.6 \times 10^{-6} A_{sc} \sqrt{f_c'}$		f_y: Yield strength of reinforcement
Hosaka et al. [12]	$V_u = 4.3A - 39 \times 10^3$	for $17 \times 10^3 < A < 152 \times 10^3$	n: Number of the hole
		$A = 0.25\pi D^2 \sqrt{t_{sc}/_D} f_c'$	d_s: Diameter of transverse rebar
	$V_u = 1.85A - 26 \times 10^3$	for $40 \times 10^3 < A < 383 \times 10^3$	A_{sc}: Shear area of concrete dowels
		$A = 0.25\pi(D^2 - d_s^2) f_c' + 0.25\pi d_s^2 f_u$	f_u: Ultimate strength of reinforcement

Table 7
Comparisons between calculated and experimental results.

Specimen code	The test V_{test}/kN	The calculated shear capacity V_{cal}/kN and the relative error						
		Leonhardt et al. [2]	Hans-Peter [4]	Oguejiofor and Hosain [6]	Ahn et al. [7]	Al-Darzi et al. [9]	Vianna et al. [11]	Hosaka et al. [12]
C-b0r1d1	449	443 / −1%	392 / −13%	270 / −40%	324 / −28%	299 / −33%	340 / −24%	414 / −8%
C-b1r1d1	547	443 / −19%	392 / −28%	270 / −51%	324 / −41%	299 / −45%	340 / −38%	414 / −24%

where:

τ_{cv} The shear strength of the concrete under multiaxial stresses (MPa);

A_c The sectional area of the concrete dowel, and $A_c = \pi(D^2 - d_s^2)/4$, D — The diameter of the hole (mm), and d_s — The diameter of the transverse rebar through the hole (mm).

The strength of the concrete under direct shear can be found by [26].

$$\tau_c = 0.25 f_c \tag{8}$$

where:

τ_c The direct shear strength of the concrete (MPa);

f_c The prismatic strength of the concrete (MPa).

Considering that the shear strength of the concrete dowel in the PBL would be improved by the confinement effect from the hole and the lateral compressive stress [16,17], here a strength enhancement coefficient ψ_c is introduced, and the relative shear strength of the concrete can be expressed by Eq.(9) with $f_c = 0.8 f_{cu}$ [24].

$$\tau_{cv} = 0.2 \psi_c f_{cu}. \tag{9}$$

Then, the resistance of the concrete dowel through the hole can be obtained as the following

$$V_{cv} = 0.4 \psi_c A_c f_{cu}. \tag{10}$$

According to the present experimental results, the contribution of the concrete dowel F_{cv} is 154 kN (see Table 5) when D, d_s and f_{cu} are 60 mm, 20 mm and 58.1 MPa, respectively. Therefore, the value of $\psi_c = 2.64$ can be obtained. The resistance of the concrete dowel through the hole can be calculated by:

$$V_{cv} = 1.06 A_c f_{cu}. \tag{11}$$

III) Resistance of the transverse rebar in the hole

The transverse rebar in the hole is subjected to the combined action of tension, bending moment and shear. Fig. 10 shows the situation of the transverse rebar in a standard PBL connector.

Similar to the calculations for the concrete dowel, the contribution of the transverse rebar can be defined as:

$$V_{sv} = 2 f_v A_s \tag{12}$$

where:

f_v The shear strength of the transverse rebar (MPa);

A_s The sectional area of the transverse rebar, and $A_s = \pi d_s^2/4$.

The shear strength of the transverse rebar can be calculated by its yield strength f_y:

$$f_v = f_y / \sqrt{3}. \tag{13}$$

As shown in Fig. 10, the transverse rebar presented typical bending-shear deformation, and the local concrete under rebar helps to increase the capacity of the connector. Because the effect of the local concrete is related to the deformation of the rebar, a coefficient ψ_s is introduced to calculate the contribution of the transverse rebar:

$$V_{sv} = 1.15 \psi_s A_s f_y. \tag{14}$$

According to the present experimental results, the contribution of the concrete dowel F_{sv} is 256 kN (see Table 5) when d_s and f_{cu} are 20 mm and 58.1 MPa, respectively. Therefore the value of $\psi_s = 1.82$ can be obtained. The resistance of the transverse rebar in the hole can be calculated by:

$$V_{cv} = 2.09 A_s f_y. \tag{15}$$

Therefore, the ultimate shear capacity of a standard PBL connector can be calculated by:

$$V_u = \tau_b A_b + 1.06 A_c f_{cu} + 2.09 A_s f_y. \tag{16}$$

4.3. Validation of the proposed equation

The related experimental results obtained separately by the third parties Q.T Su et al. [19], Zhang Q.H. et al. [20], Xiao L. et al. [21], Wu W.M. [22], and Eiichi T. et al. [27] were introduced to verify the accuracy of the proposed Eq. (16). The concrete strength of these push-out specimens varies from 35.7 MPa to 58.9 MPa, and the ratio of dowel area
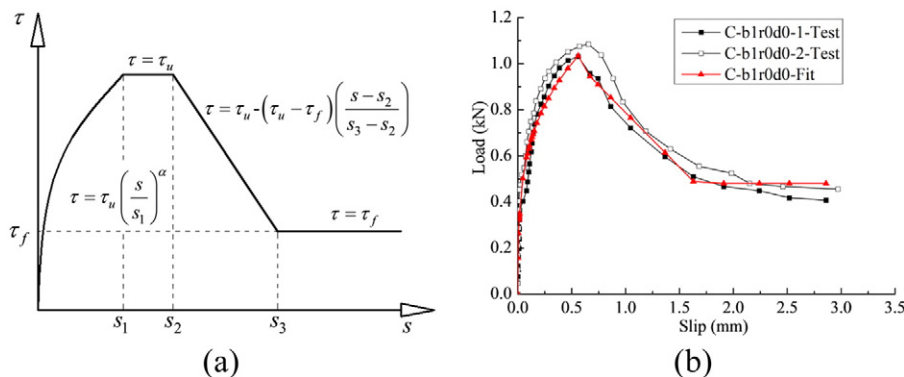

Fig. 8. The bond–slip relation between flat steel plate and concrete: (a) CEB-FIP MC90 bond–slip model; (b) Fitting results of the bond–slip curve in this work.
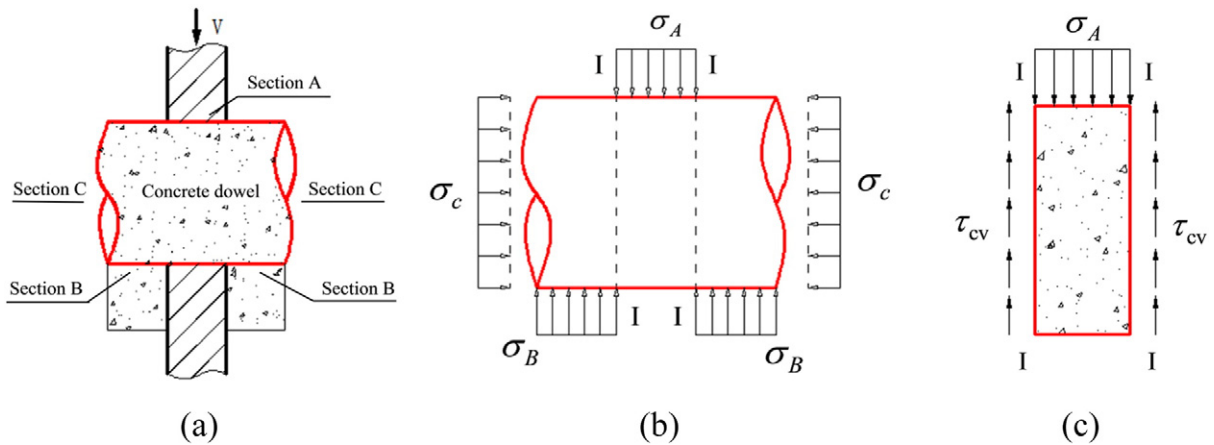
Fig. 9. Analytical diagram for concrete dowel: (a) Concrete dowel by the hole; (b) Stress diagram of concrete dowel; (c) Concrete dowel in shear.

to interfacial bonding area is between 0.02 and 0.13. It is noted that all the test results were from PBL specimens with the same failure mode as in present test, namely, the dowel being sheared off. Fig. 11 shows the comparison of the experimental and predictive results. The mean value and the standard deviation are 1.03 and 0.01, respectively; the co-efficient of determination and the Pearson Correlation Coefficient are 0.98 and 0.99, respectively, which demonstrates that proposed Eq. (16) can predict the shear-resistant capacity of PBL connectors in steel–concrete joints of hybrid bridges well.

5. Conclusions

This paper presents a study of the performance of perfobond strip connectors in steel–concrete joints by push-out tests on twelve plug-in type push-out specimens, which is different from the separated type of standard push-out specimen in EC. 4. Based on the results, the following conclusions can be drawn:

The steel plates in all types of connectors are pushed out from the concrete and the dowels in the holes in the steel plate are fractured at the end of the experimental procedure. The shear-resistant capacity of a PBL connector consists of the bonding effect at the steel plate/concrete interface and the resistance of the concrete and the rebar dowel in the hole. The bonding effect at the interface can improve the shear capacity of PBL connector, and the test results indicate that the maximum and residual bonding strengths between steel plate and the C50 concrete were 1.06 MPa and 0.51 MPa, respectively. The concrete dowel in the hole helps to transfer the loads from the steel plate to the transverse rebar inside the concrete dowel; with the concrete dowel surrounding the transverse rebar, the ultimate shear capacity of a PBL connector was significantly improved; the contribution of the concrete dowel is 28% of the overall capacity in a standard PBL connector in this work. For the PBL connector with a transverse rebar in the hole, the ultimate shear resistance and the bulk of the ultimate deformability of the connector were contributed by the action of the transverse rebar.

The shear-resistant capacity of the PBL connectors with the failure mode of dowel fracture cannot be evaluated well by the existing equations developed for connectors with failure occurring in the concrete slab. Using these equations to predict the shear capacity of the standard PBL connector in this study, the relevant predictive errors between the calculated and measured capacities range from 19%–51%. To yield better capacity estimation for the PBL connectors in the steel–concrete joints
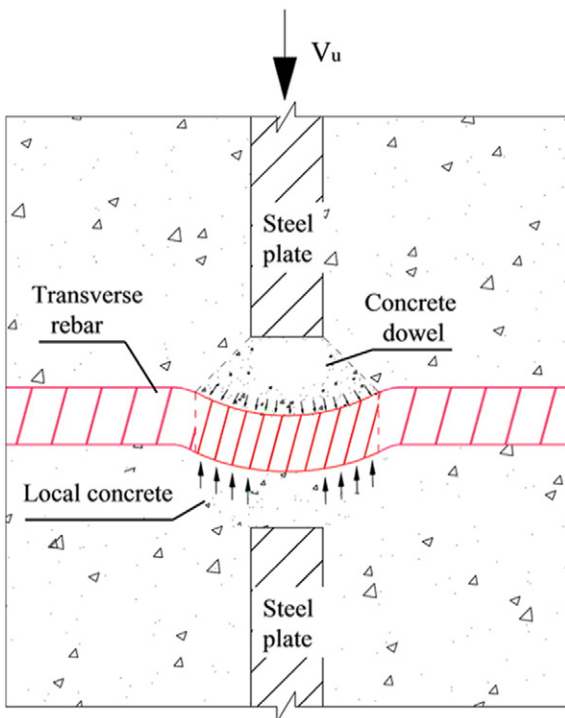

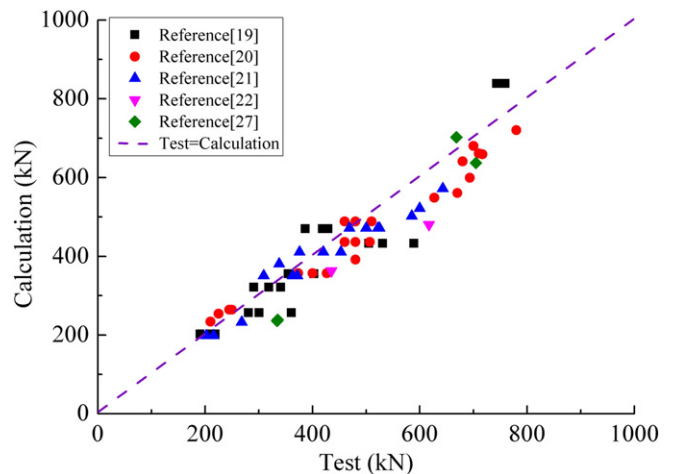**Fig. 10.** Stress diagram for transverse rebar.

Fig. 11. Comparison between tests and calculations.

of hybrid bridges, an analytical model for predicting the shear-resistant capacity of PBL connectors is developed. The model is verified by the experimental results and can be used to predict the ultimate shear–shear resistant capacity of PBL connectors in the steel–concrete joints of hybrid bridges.

Furthermore, because multiple PBL connectors are usually set in the steel–concrete joints of hybrid bridges, the interaction between the PBL connectors would prevent the shear capacity of the multiple connectors from reaching the sum of the resistances of the individual PBL connectors. As such, it is necessary to perform additional push-out tests for the case of multiple PBL connectors. Moreover, since shear connectors in steel–concrete joints of hybrid girder bridges are inevitably subjected to repeated stresses caused by traffic loads, the fatigue behavior of PBL connectors also needs to be further investigated.

Acknowledgments

References

[1] E.C. Oguejiofor, M.U. Hosain, Behaviour of perfobond rib shear connectors in composite beams: full-size tests, Can. J. Civ. Eng. 19 (2) (1992) 224–235.
[2] F. Leonhardt, W. Andra, H.-P. Andra, et al., New, improved bonding means for composite load bearing structures with high fatigue strength, Beton-Stahlbetonbau 82 (12) (1987) 325–331.
[3] EUROCODE 4. EN 1994-1-1, Design of Composite Steel and Concrete Structures Part 1.1 General Rules and Rules for Buildings, CEN-European Committee for Standardization, Brussels, 2005.
[4] Hans-Peter, Economical shear connectors with high fatigue strength, International Association for Bridge and Structural Engineering, Iabse Symposium Brussels 1990, pp. 167–172.
[5] E.C. Oguejiofor, M.U. Hosain, Parametric study of perfobond rib shear connectors, Can. J. Civ. Eng. 21 (1993) 614–625.
[6] E.C. Oguejiofor, M.U. Hosain, Numerical analysis of push-out specimens with perfobond rib connectors, Comput. Struct. 62 (4) (1997) 617–624.
[7] J.-H. Ahn, C.-G. Lee, J.-H. Won, et al., Shear resistance of the perfobond-rib shear connector depending on concrete strength and rib arrangement, J. Constr. Steel Res. 66 (10) (2010) 1295–1307.
[8] S.B. Medbery, B.M. Shahrooz, Perfobond shear connectors for composite construction, Eng. J. 39 (1) (2002) 2–12.
[9] S.Y.K. Al-Darzi, A.R. Chen, Y.Q. Liu, Finite element simulation and parametric studies of perfobond rib connector, Am. J. Appl. Sci. 4 (3) (2007) 122–127.
[10] J.d.C. Vianna, L.F. Costa-Neves, et al., Experimental assessment of perfobond and T-perfobond shear connectors' structural response, J. Constr. Steel Res. 65 (2) (2009) 408–421.
[11] J.d.C. Vianna, S.A.L. de Andrade, P.C.G.d.S. Vellasco, L.F. Costa-Neves, Experimental study of Perfobond shear connectors in composite construction, J. Constr. Steel Res. 81 (2013) 62–75.
[12] T. Hosaka, K. Mitsuki, H. Hiragi, Y. Ushijima, Y. Tachibana, H. Watanabe, An experimental study on shear characteristics of perfobond strip and its rational strength equations, J. Struct. Eng. JSCE 46A (2000) 1593–1604.
[13] H.-Y. Kim, Y.-J. Jeong, Experimental investigation on behavior of steel–concrete composite bridge decks with perfobond ribs, J. Constr. Steel Res. 62 (5) (2006) 463–471.
[14] J.P.S. Candido-Martins, L.F. Costa-Neves, P.C.G.d.S. Vellasco, Experimental evaluation of the structural response of perfobond shear connectors, Eng. Struct. 32 (8) (2010) 1976–1985.
[15] J. Hegger, M. Feldmann, S. Rauscher, O. Hechler, High-performance materials in composite construction, Struct. Eng. Int. 4 (2009) 438–446.
[16] I.B. Valente, P.J.S. Cruz, Experimental analysis of perfobond shear connection between steel and lightweight concrete, J. Constr. Steel Res. 65 (10) (2004) 465–479.
[17] I.B. Valente, P.J.S. Cruz, Experimental analysis of shear connection between steel and lightweight concrete, J. Constr. Steel Res. 60 (3) (2009) 465–479.
[18] J. He, Y. Liu, B. Pei, Experimental study of the steel–concrete connection in hybrid cable-stayed bridges, J. Perform. Constr. Facil. 28 (3) (2014) 559–570.
[19] S. Qing-Tian, W. Wang, H.-W. Luan, G.-T. Yang, Experimental research on bearing mechanism of perfobond rib shear connectors, J. Constr. Steel Res. 95 (2014) 22–31.
[20] Q.-h. Zhang, Q. Li, L. Tang, Fracture mechanism and ultimate carrying capacity of shear connectors applied for steel–concrete joint segment of bridge pylon, China J. Highw. Transp. 20 (1) (2007) 85–90 (In Chinese).
[21] X. Lin, Q. Shi-zhong, L. Xiao-zhen, et al., Research on mechanical performance of PBL shear connectors considering the perforated plate's thickness, Eng. Mech. 29 (8) (2012) 282–288 (In Chinese).
[22] W.-m. Wu, Research on Steel–Concrete Joint of Arch Bridge With Steel Box-Girder With Large Span, Tongji University, 2007 (in Chinese).
[23] Y. Majdi, C.-T.T. Hsu, S. Punurai, Local bond–slip behavior between cold-formed metal and concrete, Eng. Struct. 69 (2014) 271–284.
[24] Z. Guo, S. Xudong, Reinforced Concrete Theory and Analysis, Third ed. Tsinghua University Press, Beijing, 2012 (in Chinese).
[25] CEB-FIP, Model code for concrete structures. CEB Bulletin d'Information, Committee Euro international du Beton, Lausanne, Switzerland, 1993.
[26] Z. Guo, Strength and Deformation of Structural Concrete, First ed. Tsinghua University Press, Beijing, 1997 (in Chinese).
[27] T. Eiichi, S. Daisaku, K. Masaaki, Kiso river bridge design and erection, Kawada Tech. Rep., 21, Kawada Technologies, Tokyo 2002, pp. 42–47 (in Japanese).